PHYSOR 2002, Seoul, Korea, October 7-10, 2002

CALCULATING THE TUMOUR-SPECIFIC OPTIMAL SOURCE NEUTRON ENERGY FOR BORON NEUTRON CAPTURE THERAPY WITH PARTICLE PRODUCTION AND ADJOINT MONTE CARLO TECHNIQUES

V.A. Nievaart and R.L. Moss
Joint Research Centre of the European Commission
Postbus 2, 1755ZG Petten, The Netherlands
nievaart@jrc.nl ; moss@jrc.nl

J.L. Kloosterman and T.H.J.J. van der Hagen
Interfaculty Reactor Institute, Reactor Physics Department
Delft University of Technology
Mekelweg 15, 2629JB Delft, The Netherlands
kloosterman@iri.tudelft.nl ; T.H.J.J.vanderhagen@iri.tudelft.nl

ABSTRACT

This paper addresses the question as to whether it is useful to tailor the neutron energy for optimal irradiation of a specific tumour location in BNCT. Consequently, forward and adjoint MCNP calculations have been performed in a slab shaped geometry with human head tissue. In the forward mode the alpha, proton and proton recoil productions are determined for a spherical shaped tumour positioned at five locations between 40 mm and 80 mm from the surface. The proton production in cranium is high for source neutron energies up to 100 eV. Above 100 keV source neutrons the dose due to recoiling protons increases rapidly. To get the highest alpha production in the tumour at 40 mm, 5 eV source neutrons should be used, increasing to around 1 MeV for a tumour at 80 mm. These maximum alpha productions in tumours at different positions have been taken as the starting points for the adjoint calculations. The adjoint flux for a tumour at 60 mm is uniformly shaped, just as in the forward result, where the alpha production is optimal for a wide spectrum of source neutron energies.
The next steps will be to refine the used multigroup library for the adjoint calculations, to change the geometry to an ellipse-shaped head phantom and to apply the adjoint calculation to the other production components.

1. INTRODUCTION

In 1997, a collaboration funded by the European Commission started a clinical trial of Boron Neutron Capture Therapy to treat patients with brain tumours at the High Flux Reactor (HFR) in Petten, The Netherlands. The tumour that is treated is glioblastoma multiforme. This type of cancer is one of the worst kind, according to the survival perspective of the patient.
The idea behind the treatment is to break the DNA strands in the nucleus of the cancer cells with heavy alpha and lithium particles coming from the reaction $^{10}B(n,\alpha)\ ^{7}Li$. For that purpose, a special carrier

brings the isotope ^{10}B selectively into the tumour cells. One major challenge in BNCT is to improve the boron carrying compounds in order to discriminate more between cancer and healthy cells.
Currently, in BNCT, epithermal neutrons of about 10keV are used to penetrate the head. In this way the neutrons have a higher probability to reach the cancer cells through the overlying healthy tissues, such as skin and cranium. Due to the predominance hydrogen atoms, the neutrons will be scattered and thermalised within the brain. Unwanted dose contributions, due to unwanted located boron or produced secondary particles, are given to healthy tissue. The maximum allowable dose in healthy tissue is limited and reaching this limit may result in a premature end of the radiation, even if all the cancer cells have not yet been destroyed.
At Petten, the epithermal neutrons in the treatment beam are produced in the High Flux Reactor. A neutron filter, suppressing all unwanted neutron energies and photons, consists of Al, S, Ti, Cd and liquid (cryogenic) argon. Although this neutron filter is working well, the latter component is costly and requires regular maintenance. Therefore, an investigation has been started to design another neutron filter that will address these disadvantages with the ultimate goal to find an optimal filter and irradiation procedure for every specific tumour.
The Petten filter delivers neutrons with a fixed shaped energy distribution of which the average is 10keV. As mentioned earlier, from the neutronics point of view, it is optimal to deliver only thermal neutrons at concentrated spots where the cancer is localised.

In order to understand and to get an impression of what is happening in a human head phantom when it is radiated during BNCT, (forward) Monte Carlo calculations with simple slab geometry have been performed. In these calculations, using the MCNP code [1], the major dose delivering secondary particles are tracked in the slab according to the induced source neutron. New insight can be expected from adjoint Monte Carlo calculations with which it is possible to calculate backwards, the expected detector response of the source neutrons as a function of energy and direction.
To clarify: in a forward MCNP calculation, neutrons are tracked from the real physical source to a detector located somewhere in the phantom. In the adjoint mode, the expected detector responses are recorded in the opposite direction: the forward detector becomes the source, and the forward (or physical) source becomes the detector. Since the adjoint Monte Carlo technique is rather complicated, caused by normalisation problems in MCNP, it is necessary to first rely on the well-understood forward MCNP results.

2. FORWARD CALCULATIONS

2.1 PARTICLE PRODUCTION

In BNCT, there are four major dose contributors in tissue [2-4]. Firstly, there is the dose coming from the boron reaction. Each production of an alpha and a heavy lithium particle will contribute 2.3 MeV to tissue. Secondly, thermal neutrons will produce 0.6 MeV protons due to the $^{14}N(n,p)^{14}C$ reaction. This is referred to as the thermal dose in contrary to the third contribution, which is the fast dose caused by recoiling protons from collisions of fast neutrons with hydrogen. The energy of the recoiling nucleus can be between 0 eV and the energy of the incident neutron. As an average, half of the neutron energy is taken as the energy for the proton.
The maximum range in tissue of a 5 MeV proton is about 200 μm. For the alpha particle poduced by the $^{10}B(n,\alpha)$ reaction the range is even below 10 μm. For this reason we assume the energy of the alphas (and the lithium nuclides) and the protons is deposited locally. This is the reason that we choose to calculate in

MCNP the secondary particle production: The absorbed dose is directly proportional to the number of alphas and protons from the nitrogen production. The way of calculating the particle production is described in the MCNP manual [1] and is basically the integrated product of the energy dependent neutron flux and production cross section for all energies.
The last of the four dose contributors is coming from the gamma dose. Apart from the gammas that emanate of the reactor and pass unattenuated through the filter, there are the 2.2 MeV gammas produced by the $^{1}H(n,\gamma)^{2}D$ reaction in tissue. Since the linear energy transfer of gammas is very low, most of them will escape from the head leaving behind only a small fraction of their energy.
The philosophy behind the particle production calculations is to get a clear physical impression of what is happening in the head. It can help significantly in selecting optimal source neutron characteristics, if it is taken into account that every particle generated in healthy tissue is one too much. It is believed that this approach will keep the investigation surveyable and assist in setting up the 'backward' adjoint calculations.

2.2 MCNP SETUP

All the results given in this article are obtained in a slab shaped geometry with dimensions according to the MIRD5/Snyder phantom [5]. This means that there is a layer of skin (2 mm), soft tissue (3 mm), cranium (9 mm) and a very deep layer of brain tissue (25 cm). All tissue compositions and densities are from the ICRU 46 report [6]. Figure 1 shows a cross section through the centre of the geometry in which the sphere (radius of 20 mm) in the brain represents the tumour.

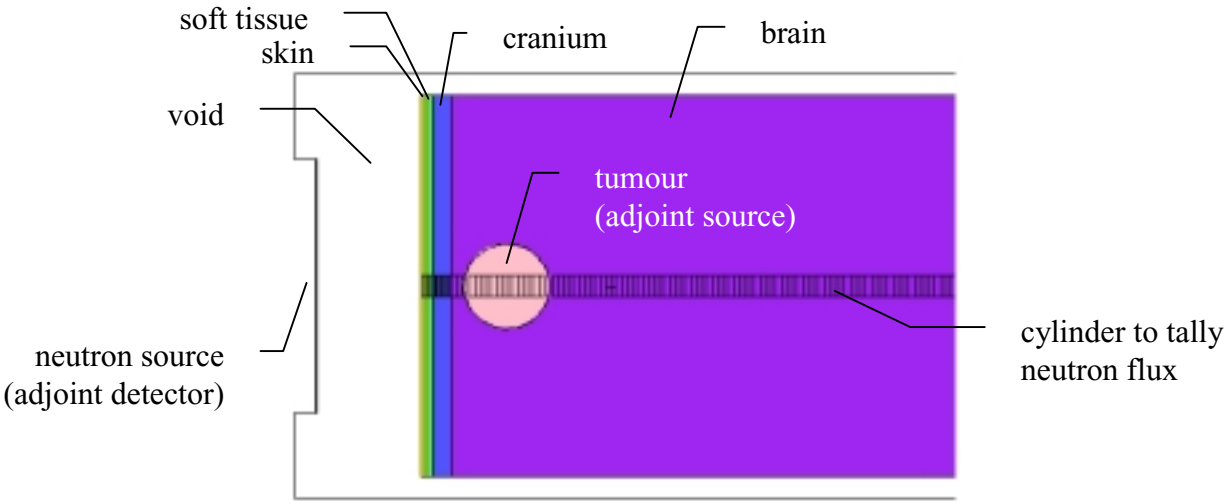

Figure 1. Cross-section of MCNP slab geometry.

The neutron flux is determined in a sliced cylinder with radius of 5 mm. The slice thickness is 2.5 mm in the brain and 1 mm elsewhere, see figure 1.
Studies in Petten [7] have shown that a ratio of 1:3 is a good representation of the ratio of ^{10}B in healthy and cancer tissue. During the calculations, 30 µg/g of ^{10}B is modelled in the tumour and 10µg/g in the rest of the head. The neutron source is disk shaped with a radius of 60 mm and emits mono-energetic and mono-directional neutrons in the energy range of 0.1 eV to 10 MeV. In this range, a total of 25 energies are logarithmically spaced.

For the calculations, the ENDF/B-VI cross-section libraries are used. In case of hydrogen the S(α,β) thermal scattering treatment is taking into account [1].

2.3 RESULTS

The plots in figures 2 to 5 are interpolated results of particle productions from the 25 discrete energies and about 56 positions in the slab. The dimension of the colour in these figures is the number of produced particles per volume and per source neutron [-/cm^3/src. n.].

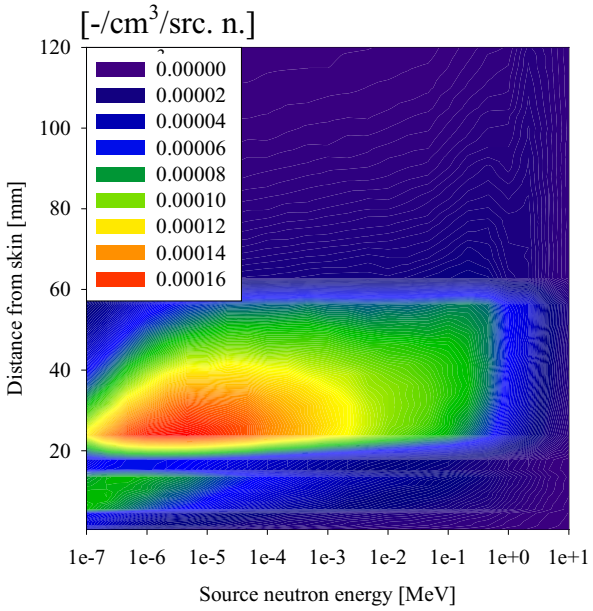

Figure 2. Alpha production with the centre of the tumour at 40 mm from the skin (tumour between 20 and 60 mm).

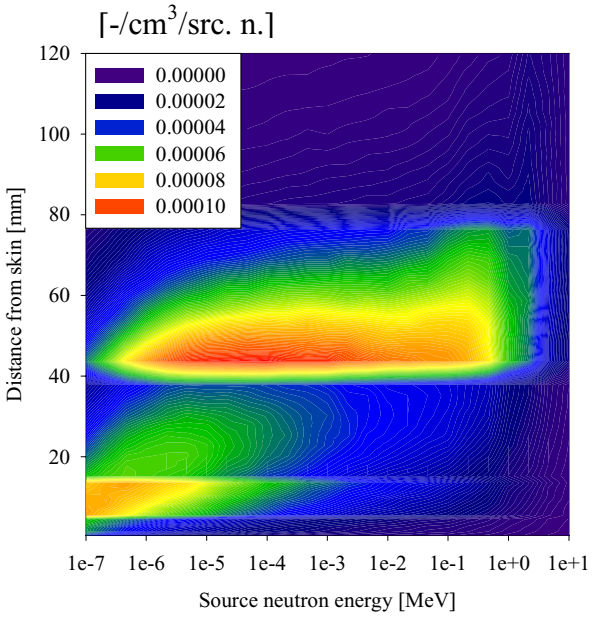

Figure 3. Alpha production with the centre of the tumour at 40 mm from the skin (tumour between 40 and 80 mm).

Figure 2 shows the alpha production (with MT number 207) as a function of the neutron source energy and the depth in the slab for a tumour at 40 mm from the skin. The boundaries of the tumour are at 20 and 60 mm, which mark the 30 μg/g ^{10}B region. For example, at neutron source energy of 1 eV: there will be $8 \cdot 10^{-5}$ alpha particles produced in the cranium (between 5 and 14 mm) for every neutron. This means on every $12 \cdot 10^{3}$ neutrons there will be one alpha particle arising. Therefore, since neutrons are already absorbed in the cranium, fewer neutrons will be available in the tumour (shielding effect). This results in a smaller red part (highest alpha production per source neutron) between the tumour boundaries as seen, for instance, when compared with source neutron energy of 10 eV. A mean neutron source energy of 10 keV, as used in most BNCT set-ups, does not give an alpha production that has its maximum in the tumour; although there is no activation in the overlying tissues. Whereas, more significantly, the 10 eV source neutrons destroy twice as much in almost half of the tumour.

The calculation of the alpha production is repeated for the cases in which the centre of the tumour is 50 mm from the skin up to 80 mm in steps of 10 mm. For example, in figure 3, for the case with the centre of the tumour 60 mm from the skin (tumour boundaries at 40 mm and 80 mm), around 1 keV source neutrons seem optimal. Note that the scaling of the colours is different than in figure 2. Based on the

alpha production only, it can be concluded that a neutron source energy in the broad range of 10 eV to 1 MeV is desirable for tumours situated from 40 mm to 80 mm. The variability in optimum source neutron energy to tumour position suggests that a variable filter may well be desirable.

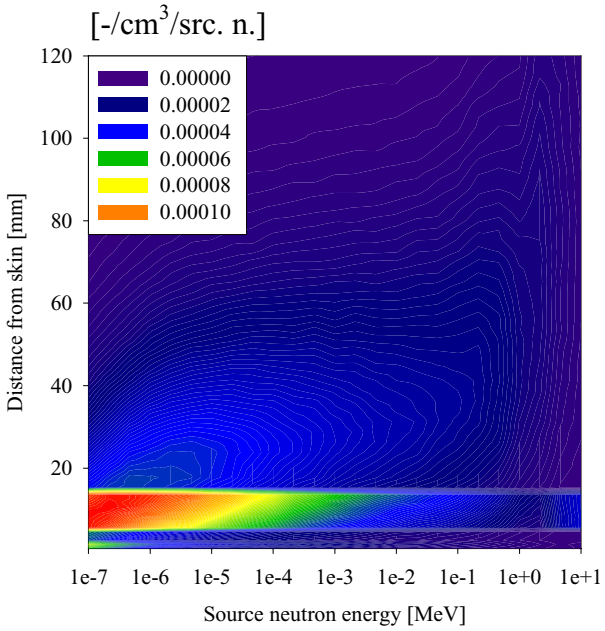

Figure 4. Proton production by nitrogen.

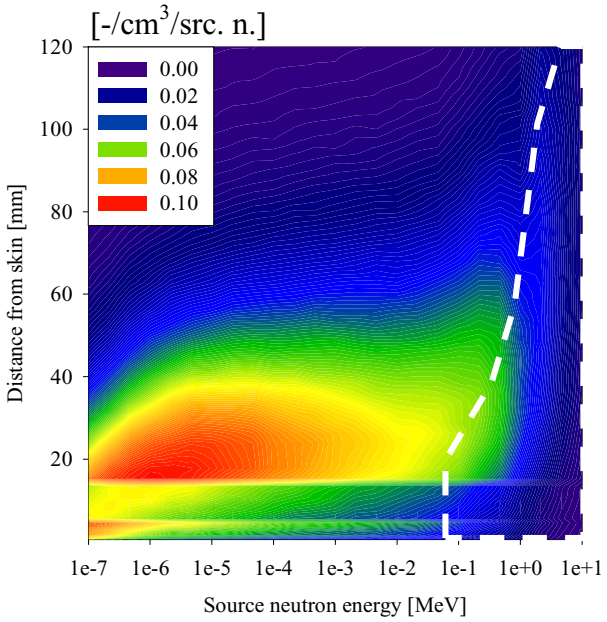

Figure 5. Recoil protons produced by hydrogen (dashed line explained in the text).

Figure 4 gives the proton production (MT203) due to nitrogen. Although the mass percentage of nitrogen in the cranium is just as high as in skin (4%), the high density of bone, roughly 1.5 greater, causes the step shaped result for source neutron energies below 1 keV. Bone is therefore a limiting factor when regarding the absorbed thermal neutron dose.

The distribution of boron has no significant influence on the proton production. This boron independence is also valid for the proton recoil outcome, as shown in figure 5. The production of recoil protons can be determined by integrating over energy the product of the neutron flux density and the elastic scattering cross section (MT2) of hydrogen. The production of recoil protons can be translated into the absorbed dose by multiplying with half of the incident neutron energy and dividing it by the tissue density. The so-called absorbed fast neutron dose is totally different when comparing it with the proton recoil production. For source neutron energies above 100 keV, the absorbed fast neutron dose will increase rapidly and penetrate deeper into the tissue. The white dashed line in figure 5 marks this area. It seems that the proton and proton recoil productions imply restrictions on the source neutron energies that can be used.

The relative errors in most of these presented results are around 3%. Not surprisingly, some errors of about 10% can be found at greater depths for low source neutron energies.

3. ADJOINT CALCULATIONS

3.1 BACKGROUND AND SETUP

The application of adjoint Monte Carlo calculations in BNCT should deliver additional insight and increased simplicity. Most of the time, adjoint calculations are done with deterministic computer codes. These codes can generate the results rather fast, but have restricted abilities concerning the geometry. Since the human head has a more complicated geometry than a slab, and because the tumour can be located anywhere, adjoint calculations using Monte Carlo with, for example, an ellipse shaped head are required. Although the calculation time is larger, Monte Carlo codes can deal with complex geometries. Two types of the adjoint Monte Carlo need to be distinguished:

- Calculation of the detector response in shielding problems, by recording in an adjoint calculation which neutrons contribute to the response function, the forward and adjoint outcome can be compared.
- Calculation of the space and energy dependent adjoint function.

With adjoint calculations, it is possible to generate more quickly, more results that are complementary with forward calculations. One has to consider all source neutron characteristics that deliver the maximum alpha production rate at all possible tumour positions in the head, whilst determining the source neutrons that cause the undesirable productions. For this purpose, the adjoint multigroup feature of MCNP can be used. In order first to know the precise capabilities and restrictions within the adjoint MCNP, the simpler slab model (see figure 1) is used. The adjoint results given in this article deal only with alpha production.

First, the forward set-up has to be transformed into the adjoint one. As indicated in figure 1, the forward source and detector are interchanged. In the adjoint run, adjoint particles that are a measure for the expected detector response will travel and ‘up-scatter’ from the tumour to the source. The changes that have to be made in the forward MCNP program listing are not difficult but the interpretation of the results is not straightforward.

3.2 NORMALISATION

An important feature to be aware of is the normalisation in MCNP: The source input data is transformed into probability densities, e.g. the spatial, angle, time and energy variables are normalised automatically to unity. As in the case of the adjoint calculation, the adjoint source is also normalised to unity and does not automatically take into account the supposed adjoint source description corresponding to the forward detector function. In general, the product of the source and response densities should be the same in the forward as well as in the adjoint case [8]. One can compensate for this normalisation artefact by determining the product of all source and response densities, except the ones automatically done by MCNP, in the forward and in the adjoint case. The correction factor follows by dividing the forward product by the adjoint one: here arises the first problem. In the forward run, a mono-directional beam is modelled. This results in a Dirac-delta function for the adjoint detector angular response. Therefore, for the sake of comparison with the forward calculation, the adjoint response function is replaced by a cosine angular one.

3.3 SCATTERING

In the adjoint calculations, the MCNP multigroup library, MGXSNP was used. The library consists of 30 energy groups between $1.39 \cdot 10^{-4}$ eV and 17 MeV. The group structure of this library is not designed for problems dominated by thermal neutrons. Significant cross-section changes in the thermal region are smeared out by the relatively large energy bin widths.
The tables for hydrogen in the multigroup library do not contain the S(α,β) thermal treatment. To investigate the importance of this, forward calculations were performed, for all the tumour positions between 40 mm and 80 mm with point-wise cross-section tables including the thermal treatment, but tallied in the 30-energy group bin structure. Comparison with the forward multigroup calculations shows that the results in the 3 lowest energy bins, between $1.39 \cdot 10^{-4}$ eV and 1.13 eV, are 1.4, 2.4 and 1.2 times higher when including the S(α,β) thermal treatment.
The lack of the thermal treatment will certainly influence the adjoint results. Currently, a new library is being investigated: one with more energy groups and thermal treatment or even applying a continuous library.

3.4 RESULTS

Figure 6 shows the results of the energy dependent adjoint function concerning the alpha production with a relative error below 3%. The tumour, which is the source in the adjoint calculation, is positioned between 40 to 80 mm (for the centre). To obtain the alpha production in the tumour, the ^{10}B absorption cross-section is used as the source function.

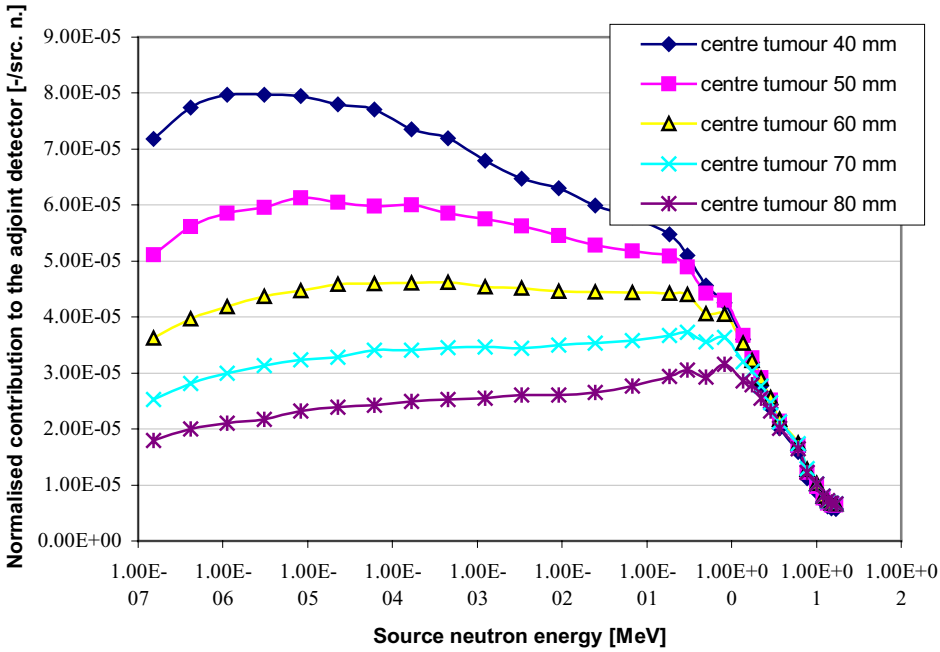

Figure 6. Adjoint function at the position of the physical source for tumours with their centre at 40 mm to 80 mm from the skin.

For a tumour of which the centre is 40 mm from the skin, around 5 eV source neutrons from the 60 mm radius source give the highest probability to contribute to the absorption reaction. The peak near to 5 eV is the result shown in figure 2: between 1 eV and 1 keV, the alpha production in the tumour 40 mm from the skin is the highest. Also the 'broadness', according to the source energy, of the alpha production for a tumour 60 mm from the skin (figure 3) is reflected in the flat shaped adjoint result.
For a tumour with the centre positioned at 80 mm from the skin, the peak is at 1 MeV, which supports the conclusion that a flexible filter can be beneficial. Comparing the yield obtained by supplying neutrons with the optimal energy with the yield from 10 keV neutrons shows that one can enhance the alpha production for the tumours positioned at 40 mm and 80 mm by 20%. For midrange-situated tumours, there is a wide range of neutron energies from which one could choose. Further, investigations, when including the unwanted effects, will probably restrict this choice.
With great prudence, it is expected that the $S(\alpha,\beta)$ thermal treatment will raise the curves with roughly 30%, since this is the average change predicted from forward calculations discussed earlier. This affects the adjoint flux at all energies and therefore the conclusions remain valid.

CONCLUSIONS

With the forward particle production calculations, the neutron reaction rates in a slab shaped head phantom have been investigated. Maximum alpha productions can be achieved for source neutron energies of 5 eV to 1 MeV for tumour depths of 40 mm to 80 mm, respectively. The restrictions in choosing source neutron energy are given by the production of protons and recoil protons by hydrogen. One can argue about the profits of having a flexible filter for BNCT, since the benefits when comparing with 10 keV neutrons is around 20% for tumours located either close to the skin or very deep in the brain.
The adjoint approach with Monte Carlo confirms the alpha production outcomes. Further investigations will use a refined multigroup library and include thermal treatment for hydrogen for the adjoint as applied to an ellipse shaped geometry. This would enable, rather quickly, to determine the neutron contribution for every point outside the skin to a tumour location within. A further challenge is to investigate whether the adjoint calculations can be used to give useful information concerning the other, unwelcome, dose contributions.

ACKNOWLEDGEMENTS

Thanks is given to D. Legrady for his input concerning the adjoint normalisation. This research is supported by the European Commission.

REFERENCES

1. J.F. Briesmeister, Ed., "MCNP – A General Monte Carlo N-Particle Transport Code, Version 4C," LA-13709-M (April 2000).
2. F.J. Wheeler, D.W. Nigg, "Three-Dimensional Radiation Dose Ditribution Analysis for Boron Neutron Capture Therapy," Nucl. Sci. Eng. 110: 16-31 (1992).
3. J.M. Verbeke, J. Vujic, and K.N. Leung, "Neutron Beam Optimization for BNCT using the D-D and D-T High-Energy Neutron Sources," Nucl. Technol. 129 (2), 257-278 (2000).

4. M.K. Marashi, “Analysis of absorbed dose distribution in head phantom in boron neutron capture therapy,” Nucl. Instr. and Methods in Physics Research A440: 446-452 (2000).
5. W.S. Snyder, M.R. Ford, G.G. Warner and H.L. Fisher Jr., “Estimates for absorbed fractions for monoenergetic photon sources uniformly distributed in various organs of a heterogeneous phantom,” J. Nucl. Med. Suppl. 3, 47 (August 1969).
6. ICRU 46, “Photon, electron, proton and neutron interaction data for body tissues,” International Commission on Radiation Units and Measurements, Bethesda, MD (1992)
7. K. Hideghéty, W. Sauerwein, R.L. Moss, R. Huiskamp, Ed.,”Tissue uptake of borocaptate sodium in patients with glioblastoma in the EORTC 11 961 phase I BNCT trial”.
8. J.C. Wagner, E.L. Redmond II, S. P. Palmtag, J. S. Hendricks, “MCNP: Multigroup/Adjoint capabilities,” LA-12704.